In situ cleaning and characterization of oxygen- and zinc-terminated, *n*-type, ZnO{0001} surfaces

B. J. Coppa, C. C. Fulton, P. J. Hartlieb, and R. F. Davis[a)]
Department of Materials Science and Engineering, North Carolina State University, Box 7907, Raleigh, North Carolina 27695

B. J. Rodriguez, B. J. Shields, and R. J. Nemanich
Department of Physics, North Carolina State University, Box 8202, Raleigh, North Carolina 27695

(Received 5 August 2003; accepted 13 February 2004)

A layer containing an average of 1.0 monolayer (ML) of adventitious carbon and averages of 1.5 ML and 1.9 ML of hydroxide was determined to be present on the respective O-terminated $(000\bar{1})$ and Zn-terminated (0001) surfaces of ZnO. A diffuse low-energy electron diffraction pattern was obtained from both surfaces. *In situ* cleaning procedures were developed and their efficacy evaluated in terms of the concentrations of residual hydrocarbons and hydroxide and the crystallography, microstructure, and electronic structure of these surfaces. Annealing $ZnO(000\bar{1})$ in pure oxygen at $600-650\,^{\circ}C \pm 20\,^{\circ}C$ reduced but did not eliminate all of the detectable hydrocarbon contamination. Annealing for 15 min in pure O_2 at $700\,^{\circ}C$ and 0.100 ± 0.001 Torr caused desorption of both the hydrocarbons and the hydroxide constituents to concentrations below the detection limits (~ 0.03 ML $= \sim 0.3$ at. %) of our x-ray photoelectron spectroscopy instrument. However, thermal decomposition degraded the surface microstructure. Exposure of the $ZnO(000\bar{1})$ surface to a remote plasma having an optimized 20% O_2/80% He mixture for the optimized time, temperature, and pressure of 30 min, $525\,^{\circ}C$, and 0.050 Torr, respectively, resulted in the desorption of all detectable hydrocarbon species. Approximately 0.4 ML of hydroxide remained. The plasma-cleaned surface possessed an ordered crystallography and a step-and-terrace microstructure and was stoichiometric with nearly flat electronic bands. A 0.5 eV change in band bending was attributed to the significant reduction in the thickness of an accumulation layer associated with the hydroxide. The hydroxide was more tightly bound to the ZnO(0001) surface; this effect increased the optimal temperature and time of the plasma cleaning process for this surface to $550\,^{\circ}C$ and 60 min, respectively, at 0.050 Torr. Similar changes were achieved in the structural, chemical, and electronic properties of this surface; however, the microstructure only increased slightly in roughness and was without distinctive features. © *2004 American Institute of Physics.* [DOI: 10.1063/1.1695596]

I. INTRODUCTION

The most common polytype of zinc oxide (ZnO) possesses the hexagonal wurtzite crystal structure, *n*-type electrical character under normal zinc and oxygen partial pressures,[1] and a direct band-gap energy at room temperature of 3.4 eV.[2] Applications for bulk polycrystalline and powdered ZnO include surface acoustic wave devices, gas sensors, piezoelectric transducers, varistors, transparent conducting films for the photovoltaic industry, phosphors, and pigments in paints.[3] Recent interest and research in this material have focused on its potential for (1) electro-optical applications including blue and ultraviolet light-emitting diodes and lasers as well as ultraviolet detectors and (2) spintronics applications via the introduction of Mn to produce oxide-diluted magnetic semiconductors.[4] Advances in the development and commercialization of large-area ZnO substrates for the homoepitaxial growth of films and device structures provides a significant advantage relative to the III-nitrides, the principal competitor materials. A review of the recent advances in ZnO materials, their properties, and devices has recently been published.[1]

Surface cleaning processes are fundamental to semiconductor device fabrication.[5] Previous studies[6–8] have shown that the removal of contaminants from the surfaces of silicon- and gallium arsenide-based substrates decreases both the concentration of growth-related zero- and one-dimensional defects in the subsequently deposited epitaxial films and the reverse bias leakage current in rectifying contacts, and enhances device functionality.[5] Similar gains in the microstructure and electrical properties should be realized in homoepitaxial films of ZnO grown on clean ZnO substrates; however, only a few reports regarding contaminant removal from ZnO surfaces have been published.[9–12]

Initial cleaning studies of ZnO single crystals were performed by Fiermans *et al.*[9] using chemical etching and annealing under an unspecified ambient and pressure. The results of x-ray photoelectron spectroscopy (XPS) and Auger electron spectroscopy (AES) of the $ZnO(000\bar{1})$ surfaces revealed traces of residual S and Cl from the chemical treatments in H_2SO_4 and HCl, respectively. Additional AES

a)Author to whom correspondence should be addressed; electronic mail: robert_davis@ncsu.edu

spectra indicated that annealing at 700 °C for 10 min resulted in significant oxygen desorption, the removal of all detectable carbon, and the outdiffusion of Ca impurities. Low-energy electron diffraction (LEED) revealed the formation of a (1×1) hexagonal pattern with spots of peculiar symmetry, which were attributed to thermal etching. Application of this same cleaning procedure to the ZnO(0001) face resulted in stronger XPS and AES signals for S, Cl, and Ca, and a weaker (1×1) hexagonal LEED pattern. Thus, these processes are neither suitable for wafer cleaning nor compatible with standard device processing procedures.

Jacobs and co-workers[10] determined from AES spectra that annealing ZnO$(000\bar{1})$ at 597 °C in 3×10^{-3} Torr of O_2 for 30 min reduced the carbon concentration on the surface. A more defined (1×1) LEED pattern was also obtained. However, removal and/or characterization of the surface hydroxide was not reported.

Several groups have utilized Ar^+ bombardment from an ion gun followed by annealing for the removal of surface contamination from ZnO. XPS results acquired by Mintas and Filby[11] from the surface of as-received sintered ZnO tablets revealed both the hydroxide component of the O 1*s* core level located 1.5–2 eV higher in binding energy than lattice oxygen and a significant concentration of carbon, as determined from the analysis of the C 1*s* core level. Exposure to 6 kV Ar^+ ions in a beam current of 40 μA for 20 min removed all detectable concentrations of these contaminants.[11]

AES spectra obtained by Roberts and Gorte[12] revealed the removal of C impurities from the {0001} surfaces of ZnO single crystals after exposure to Ar ions and subsequent annealing in a vacuum at 527 °C for 30 min and at 427 °C for 30 min in O_2 at 1×10^{-8} Torr. Hydroxide removal was not discussed, since only AES was used as a characterization tool and, in this instrument, the oxidation states of the oxygen are not readily distinguished. In general, ion bombardment typically results in the physical and chemical alteration of the surface and the underlying layers through mixing, roughening, formation of craters, and/or a change in oxidation state.[11]

It has been proposed[13] that each H atom donates $\sim0.5e^-$ to each surface oxygen atom on the hydroxylated (0001) and $(000\bar{1})$ surfaces of ZnO. This strong interaction, comparable to O–metal bonding in the bulk oxide lattice, can purportedly result in the formation of a shallow electron donor state through the proposed reaction: $(H+O^{2-}\rightarrow OH^-+e^-)$ and increase the carrier concentration in the space-charge layer by several orders of magnitude.[13] As such, several groups have reported that the hydroxide leads to the formation of an accumulation layer that results in a high surface conductivity on both polar faces of ZnO.[14–16]

In our study, *in situ* cleaning procedures involving annealing in either oxygen or a remote O_2/He plasma were investigated for the removal of adventitious hydrocarbons and hydroxide from the polished {0001} faces of ZnO wafers. The efficacy of these procedures was determined using several *in situ* spectroscopy, microstructural, and structural characterization techniques, as described in the following sections.

II. EXPERIMENTAL PROCEDURES

Two millimeter thick, grade II, single-crystal ZnO$(000\bar{1})$ and ZnO(0001) wafers, diced from boules produced by seeded chemical vapor transport by Eagle–Picher Technologies, Incorporated,[17] and chemomechanically polished on both sides, were employed in the present research. Hall and capacitance–voltage measurements, the latter at 1×10^4 Hz, taken from the $(000\bar{1})$ surface of the as-received wafers, showed a bulk carrier concentration of $1\pm5\times10^{17}$ cm^3 and a nominal effective donor concentration, (N_D-N_A), of $5\pm5\times10^{16}$ cm^3, respectively. The wafers were cleaved into smaller sections, rinsed *ex situ* in methanol for 5 s, and dried in flowing nitrogen. *Ex situ* exposure of the samples to a UV/ozone environment for 15 min reduced the hydrocarbon concentration below the detection limit of AES. However, this method was not further employed due to the persistent photoconductivity of ZnO when exposed to UV light, as reported previously.[18,19] Samples were stored in a dessicator under ~1 Torr vacuum with packets of humidity sponges that were replaced monthly. This procedure minimized further reaction with water vapor and the continued formation of the hydroxide.

All *in situ* metal deposition, cleaning, and surface characterization experiments were conducted within a ultrahigh vacuum (UHV) configuration,[20] which integrates several independent cleaning, thin-film growth, and analysis systems via a transfer line having a base pressure of 1×10^{-9} Torr. The initial process step was the deposition of an ~40 nm thick Ti film via electron-beam evaporation on the entire (0001) or $(000\bar{1})$ face of each ZnO piece. This film served to absorb radiation from the underlying heater (see below) and to conduct heat into the wafer during the cleaning of the opposite face. Each ZnO sample was subsequently mounted with Ta wires onto an Inconel® holder that was transferred to a larger Inconel® holder located 40 cm below the center of a rf coil in a remote plasma chamber, having a base pressure of 5×10^{-9} Torr.

Heating of the sample was achieved with a stage consisting of a wound 70% platinum–30% rhodium heating filament mounted on a boron nitride disk that was supported by three alumina tubes. Heating profiles were controlled with a 20 A semiconductor current rectifier power supply. A chromel–alumnel (*K*-type) thermocouple with an Inconel® sheath located in close proximity to the sample was used to measure the temperature. An optical pyrometer with a spectral response of 0.96–1.05 μm was used to calibrate the heater for the extrapolation of temperatures above 600 °C. An emissivity of 0.64 was programmed for the titanium film noted above. The uncertainty in all temperature measurements was ±20 °C.

Two different investigations were conducted to remove the hydrocarbon and hydroxide contaminants from the ZnO surfaces: (1) Annealing ZnO$(000\bar{1})$ in flowing oxygen and (2) exposure of both ZnO$(000\bar{1})$ and ZnO(0001) to a remote oxygen plasma at elevated temperatures. In the former study,

TABLE I. Experimental sets of temperature, total pressure, and time parameters investigated to determine the efficacy of annealing ZnO$(000\bar{1})$ in pure O_2 for the removal of surface contaminants.

Experiment No.	Sample temperature ($\pm 20\,^{\circ}$C)	Process pressure (± 0.001 Torr)	Process time (min)
1	600	0.100	30
2	625	0.100	30
3	650	0.100	30
4	700	0.100	15
5	700	0.100	30

each sample was heated at a rate of a $\sim 20\,^{\circ}$C/min to 300 °C. Pure oxygen was subsequently flowed through the system at 300 °C to produce a constant pressure of 0.100 Torr, which was regulated using a turbomolecular pump. The selected sample was then heated at 30 °C/min to a single annealing temperature of 600 °C, 625 °C, 650 °C, or 700 °C; held for the time associated with that temperature, as shown in Table I, and cooled at 30 °C/min to 300 °C. The system was then evacuated and the sample was cooled to room temperature.

The remote plasma was achieved by exciting mixtures of research-grade helium and oxygen, containing, in the majority of the experiments, 20 vol % of the latter gas, via the flow of 15 sccm of O_2 and 60 sccm of He through a quartz tube mounted at the top of the chamber. The tube was surrounded by a copper coil connected to a tuned 20 W power supply operated at 13.56 MHz. The ZnO samples were processed at $\sim 20\,^{\circ}$C, 350 °C, 450 °C, 475 °C, 500 °C, 525 °C, 575 °C, or 600 °C, and the heating rate was $\sim 20\,^{\circ}$C/min. The gas mixture was introduced into the system when the sample temperature reached 425 °C (except for the 20 °C and 350 °C exposures where the gases were introduced at those temperatures) before striking the plasma. It was determined that heating ZnO in a vacuum to 425 °C did not generate surface degradation; thus, this temperature was chosen thereafter for the introduction of the gas mixture into the chamber. Plasma exposure times ranged from 0.5–60 min (see Tables II and III). The samples exposed to the plasma at the high temperatures were cooled in the plasma ambient to 425 °C and subsequently in a vacuum (all samples) below this temperature.

A 3 kV beam voltage and 1 mA filament current were used in the AES analyses. Spectra were collected in the undifferentiated mode and numerically differentiated. A constant 2 mA filament current was used to obtain the LEED patterns; however, it was necessary to vary the beam voltages between 20–100 eV because of the varying amounts of surface contamination.

All XPS spectra were acquired, typically over a period of 1 h, using a Mg $K\alpha$ source ($h\nu = 1253.6$ eV) operated at 13 kV and 20 mA emission current in tandem with a hemispherical electron energy analyzer with a mean radius of 100 mm (VG CLAM II). Periodic scans of the Au $4f_{7/2}$ peak of a gold standard made by electron-beam evaporation on a Si(100) wafer allowed corrections to be made for discrepancies from the known value of 84.0 eV.[21] The data were most accurately represented by a mixed Gaussian–Lorentzian peak shape with a linear background, which was systematically subtracted from the initial spectra.

An Omicron HIS 13 vacuum UV discharge lamp powered by a NG HIS power supply and emitting He I 21.2 eV radiation was used in conjunction with an angle-resolved UV photoelectron spectrometer (ARUPS) with a base pressure of 5×10^{-10} Torr to to obtain spectral information regarding the electronic structure of the ZnO surface. A 500 V potential, a 50 mA discharge current, and a 4 V sample bias were used in these studies. Helium which leaked into the ARUPS from the lamp inlet raised the pressure of the chamber to $\sim 1 \times 10^{-8}$ Torr during operation; however, this inert environment did not produce surface contamination. A VSW HA50 50 mm radius hemispherical electron energy analyzer having

TABLE II. Experimental sets of sample and remote 20 W plasma parameters investigated for the removal of surface contaminants from the ZnO$(000\bar{1})$ surface. The Zn/O ratios are those attained after cleaning. The change in band bending associated with the use of each set of parameters is indicated by $\Delta(q\Psi_s)$. The optimum cleaning procedure and associated results are shown in bold.

Exp. No.	Sample temp. ($\pm 20\,^{\circ}$C for $T >$ RT)	O_2/He vol % ratio in plasma	Plasma pressure (± 0.001 Torr)	Plasma exposure time (min)	Thickness initial OH layer (± 0.1 ML)	Thickness residual OH layer (± 0.1 ML)	Zn/O ratio (± 0.1)	$\Delta(q\Psi_s)$ (± 0.1 eV)
1	~ 20	2/98	5.0	0.5	1.7	1.70	0.4	0.1
2	~ 20	2/98	0.050	0.5	1.7	1.7	0.4	0.1
3	~ 20	2/98	0.050	1.0	1.7	1.7	0.4	0.1
4	350	12/88	0.050	0.5	1.4	0.9	0.5	0.3
5	450	12/88	0.050	0.5	2.6	1.7	0.4	0.5
6	475	20/80	0.050	0.5	1.7	0.9	0.8	0.6
7	500	20/80	0.050	2.0	1.6	0.9	0.5	0.6
8	525	20/80	0.050	0.5	1.4	0.7	0.4	0.5
9	525	20/80	0.050	15	1.3	0.6	0.9	0.4
10	**525**	**20/80**	**0.050**	**30**	**1.6**	**0.4**	**1.0**	**0.5**
11	525	20/80	0.050	45	1.6	0.4	1.0	0.5
12	575	20/80	0.050	0.5	0.9	0.0	0.9	0.4
13	600	20/80	0.050	1	1.3	0.0	0.7	0.6
14	600	20/80	0.050	15	0.7	0.0	0.7	0.3

TABLE III. Experimental sets of sample and remote 20 W plasma parameters investigated for the removal of surface contaminants from the ZnO(0001) surface. The Zn/O ratios are those attained after cleaning. The change in band bending associated with the process is indicated by $\Delta(q\Psi_s)$. The optimum cleaning procedure and related results are shown in bold.

Exp. No.	Sample temp. (± 20 °C)	O_2/He vol % ratio in plasma	Plasma process pressure (± 0.001 Torr)	Plasma exposure time (min)	Thickness initial OH layer (± 0.1 ML)	Thickness residual OH layer (± 0.1 ML)	Zn/O ratio (± 0.1)	$\Delta(q\Psi_s)$ (± 0.1 eV)
1	525	20/80	0.050	30	2.0	1.6	0.5	0.5
2	525	20/80	0.050	60	2.0	1.6	0.5	0.6
3	**550**	**20/80**	**0.050**	**60**	**1.6**	**0.4**	**1.0**	**0.6**

a four-element lens was used to collect the UV photoelectron spectrometer (UPS) results.

Atomic force microscopy (AFM) of the surface microstructure, before and after the cleaning experiments, was performed primarily in the contact mode to determine if the cleaning procedures introduced surface damage from thermal decomposition and chemical and/or mechanical interactions with the plasma species. A commercially available PSI M5 system and silicon and/or silicon nitride tips were used for this study.

The following sections present, discuss, and summarize the effects of exposure to either thermal annealing or an O_2-containing plasma for the removal of hydrocarbons and hydroxyls from the ZnO{0001} surfaces. It is important to note that all wafers will have been *ex situ* cleaned in the manner noted above prior to loading into UHV for the *in situ* cleaning and the subsequent photo-optical and electron-beam investigations of the efficacy of these cleaning routes, unless indicated otherwise. These samples are referred to as either ''*ex-situ* cleaned'' or ''as-loaded'' in the following sections.

III. RESULTS AND DISCUSSION

A. Contaminants on the as-received and *ex-situ* cleaned surfaces

AES and XPS scans showed hydrocarbons and hydroxyls to be the only measurable contaminants on the as-received and *ex situ* cleaned ZnO(0001) and ZnO$(000\bar{1})$ surfaces of all the samples investigated in this research. Calculations based primarily on the XPS spectra indicated that the contamination layer on both basal planes of the as-loaded ZnO samples contained at least 1.0 ± 0.1 monolayer (ML) of hydrocarbon species and from 0.7 ± 0.1 ML to 2.6 ± 0.1 ML of hydroxide; this is in agreement with other reports.[10,22] All LEED patterns acquired with an incident beam energy $\leqslant 100$ eV from the *ex situ* cleaned surfaces were diffuse, which was attributed to the amorphous hydroxide layer.

B. Oxygen annealing of ZnO$(0001\bar{})$ surface

The process parameters and the results of the investigations by Jacobs *et al.*[10] noted above provided the initial conditions for the annealing experiments in this study. The primary focus of much of this component of the research concerned the complete removal of the hydrocarbon species. No measurable removal of this contaminant was indicated by a comparison of the C*KLL* AES peaks acquired from the ZnO$(000\bar{1})$ surface of the *ex situ* cleaned sample [see spectrum (i) in Fig. 1] with that acquired from the same sample annealed at 600 °C for 30 min in 0.100 Torr of flowing oxygen (Exp. No. 1, Table I). Annealing at 625 °C (Exp. No. 2, Table I) resulted in a 20% reduction in intensity of the C*KLL* AES peak. Increasing the annealing temperature to 650 °C (Exp. No. 3, Table I) allowed a well-defined (1×1) hexagonal LEED pattern to be obtained using a primary beam potential of 20 eV. This was apparently due to the desorption of some of the hydroxide, as the intensity of the C*KLL* AES peak was unchanged from that observed after the anneal at 625 °C. Moreover, carbon has been reported to only lessen the clarity of a LEED pattern for ZnO$(000\bar{1})$, indicating that it may be more ordered and/or less thick than the OH layer.[9]

Annealing at 700 °C for 15 min (Exp. No. 4) resulted in a similar LEED pattern at 20 eV and increases in the inten-

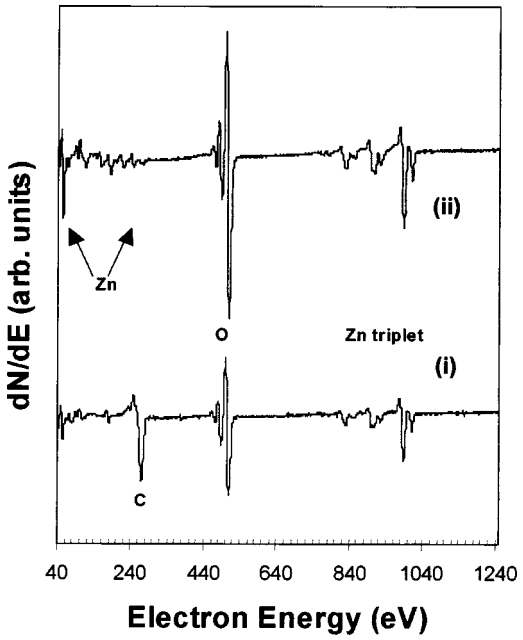

FIG. 1. AES spectra of the ZnO$(000\bar{1})$ surface acquired from (i) an *ex situ* cleaned sample and (ii) a sample annealed in 0.100 Torr of pure O_2 at 700 °C for 15 min (Exp. No. 4, Table I).

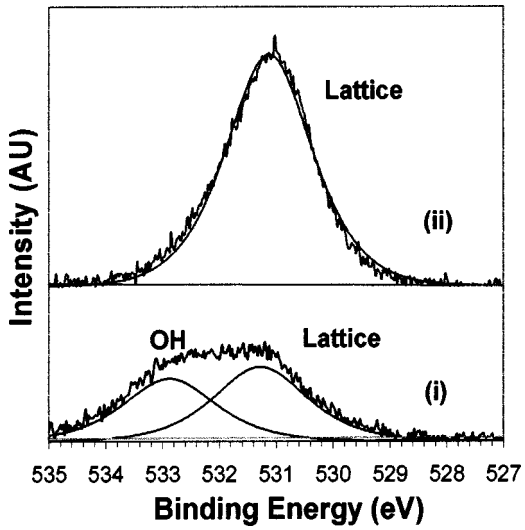

FIG. 2. XPS O 1*s* core-level spectra of the ZnO$(000\bar{1})$ surface acquired from (i) an as-loaded sample and (ii) a sample annealed in 0.100 Torr of pure O_2 at 700 °C for 15 min (Exp. No. 4, Table I). The straight lines through each spectrum represent a linear baseline.

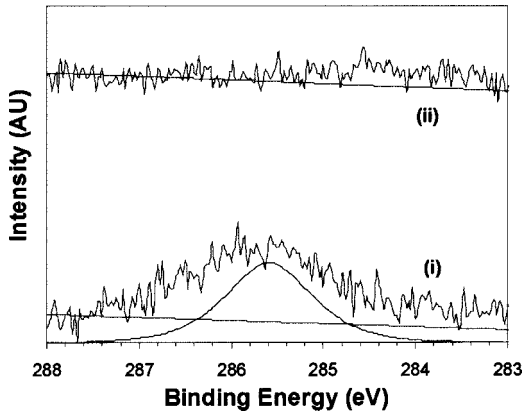

FIG. 3. XPS C 1*s* core-level spectra of ZnO$(000\bar{1})$ surfaces acquired from (i) as-loaded samples and (ii) a sample cleaned by exposure to a 20 W, 2% O_2/98% He remote plasma at room temperature for 0.5 min at 0.050 Torr. The straight lines through each spectrum represent a linear baseline.

sities of the O *KLL* and Zn *LMM* Auger peaks by 100% and 67%, respectively, as shown in spectrum (ii) in Fig. 1. The carbon signal was not detectable. Companion XPS investigations of the O 1*s* core level revealed a doublet in the spectrum for the as-loaded ZnO$(000\bar{1})$ surface, as shown in spectrum (i) in Fig. 2. The higher binding energy peak at 532.9 eV is indicative of ~2 ML of OH on this sample.[9] The XPS core-level spectra in these studies have an uncertainty of ±0.1 eV, and 1 at. % of hydroxide corresponds to 0.1 ML. Oxygen bonded to zinc in the lattice is identified at 531.3 eV, which is the lower binding energy peak in spectrum (i) in Fig. 2. The hydroxide signal is not observed after the cleaning process, as shown in spectrum (ii) in Fig. 2; this means that less than ~0.3 at. % (~0.03 ML) of the hydroxyls remain on the surface, as this value represents the detection limit of our XPS system. The lattice oxygen peak is also shifted 0.2 eV to a lower binding energy of 531.1 eV. The intensity of the C 1*s* core-level peak of the as-loaded surface, observed at 285.6 eV, decreased to below the noise level as a result of the annealing process; this confirms the carbon removal indicated by the AES spectra in Fig. 1. Furthermore, the Zn $2p_{1/2}$ core-level peak at 1045.2 eV and Zn $2p_{3/2}$ peak at 1022.1 eV were reduced in binding energy by 0.4 eV. The average value of 0.3±0.1 eV for the Zn 2*p* and O 1*s* core-level shifts is ascribed to a change in band bending associated with the cleaning process.

Extending the annealing time to 30 min (Exp. No. 5) caused decomposition and the associated formation of needles separated by ~1 μm and oriented in three crystallographic directions over the surface in a manner similar to those observed in decomposition studies of ZnO by Leonard and Searcy.[23,24] As a result, the root-mean-square (rms) surface roughness increased from 5.7±0.2 nm for the as-loaded material to 15.8±0.2 nm for the oxygen-annealed material. Further evidence of the decomposition of ZnO was deduced from the LEED pattern in that the (1×1) hexagonal pattern was replaced by a diffuse background. XPS studies revealed an increase in the Zn/O atomic ratio from 0.7±0.1 for the as-loaded surface to 1.2±0.1 for the decomposed surface, which indicates the loss of lattice oxygen and/or the diffusion of Zn to the surface. Decomposition of the ZnO$(000\bar{1})$ surface has been investigated by quadrupole mass spectrometer measurements under UHV conditions. Kohl *et al.*[25] reported that measurable sublimation in the form of atomic Zn and O from a UHV-cleaved surface begins at 600 °C.[25] Fiermans *et al.*[9] noted that annealing ZnO$(000\bar{1})$ at 700 °C and 1×10^{-10} Torr for periods greater than 10 min caused thermal etching, as indicated by the formation of (1×1) hexagonal LEED spots with peculiar symmetries. In addition, Nowok[26] reported that prolonged exposure of the ZnO$(000\bar{1})$ surface to a several-hundred-volt electron beam generated a hexagonal-to-cubic phase transformation measurable by x-ray diffraction and the formation of dendrites observed in scanning electron microscopy.

C. Remote plasma cleaning of the ZnO$(000\bar{1})$ surface

The use of remote 20 W O_2/He plasmas containing free radicals of oxygen, helium atoms, and oxygen molecules were investigated as another process route to achieve a clean, well-ordered, stoichiometric, and undamaged ZnO$(000\bar{1})$ surface. Table II summarizes the parameters used in the plasma cleaning experiments and the results gleaned from the XPS spectra before and after cleaning in ascending order of temperature. Carbon was removed below the detection limit of the XPS by every remote plasma exposure investigated, as shown, e.g., by a comparison of spectrums (i) and (ii) of the C 1*s* core level in Fig. 3. The latter spectrum was acquired at the lowest temperature of ~20 °C and the shortest exposure time of 0.5 min (Exp. No. 1, Table II). Additional XPS studies of the O 1*s* and the Zn 2*p* multiplet spectra revealed that the hydroxide coverage of ~1.7 ML and a nonstoichiometric surface with the Zn/O ratio=0.4, determined for the as-loaded sample, remained after exposure to the conditions noted for experiment Nos. 1–3 in Table II. Representative XPS O 1*s* core-level data for experiment

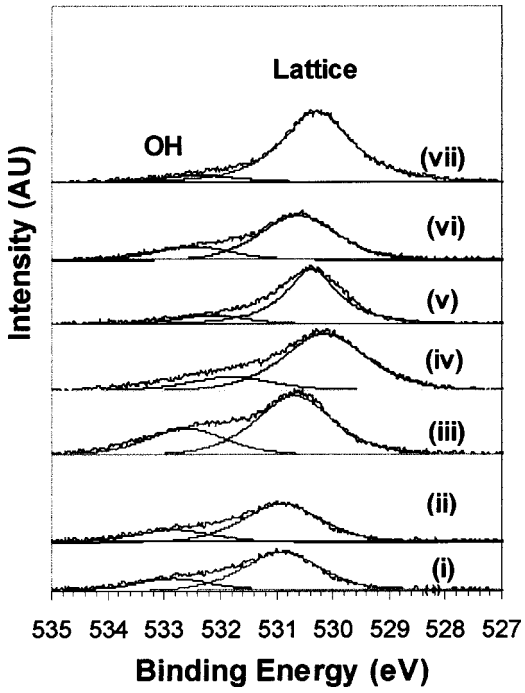

FIG. 4. XPS O 1*s* core-level spectra of ZnO($000\bar{1}$) surfaces acquired from (i) an as-loaded sample and samples separately exposed to a 20 W remote O_2/He plasma for 0.5–30 min at 0.050 Torr at (ii) 20 °C (iii) 350 °C, (iv) 450 °C, (v) 475 °C, (vi) 500 °C and (vii) 525 °C. The amount of hydroxide varied slightly for each as-loaded sample.

Nos. 2 and 3 are shown in spectrums (i) and (ii), respectively, in Fig. 4. LEED studies up to 100 eV revealed only an amorphous background similar to that observed on the as-loaded surface.

To enhance the removal of the hydroxide, it was deemed necessary to either increase the energy of the plasma and risk surface damage or to increase the temperature of the ZnO substrate and risk the evaporation that occurred in the high-temperature annealing experiments. The latter approach was selected to determine if a combination of exposure time to the remote plasma and an elevated temperature existed whereby significant removal of the hydroxide could be achieved without measurably affecting the microstructure of the substrate surface. Remote plasma exposures were conducted at elevated temperatures beginning at 350 °C (Exp. No. 4, Table II). The volume percent of O_2 in the plasma was increased to 12% to suppress the desorption of lattice oxygen from the heated ZnO($000\bar{1}$) surface. Heating the ZnO to 350 °C before exposure to the plasma reduced the hydroxide thickness by ~0.5 ML and increased the Zn/O ratio from 0.4 to 0.5, as compared to the as-loaded surface. The Zn $2p_{1/2}$ and Zn $2p_{3/2}$ XPS core-level peaks were shifted from 1044.9 eV and 1021.9 eV for the as-loaded surface to 1044.6 eV and 1021.7 eV for the plasma-cleaned surface. The O 1*s* lattice XPS peak exhibited a similar 0.3 eV change in band bending through the core-level shift from 530.6 eV for the as-loaded surface to 530.3 eV after cleaning, as shown in spectrum (iii) in Fig. 4. A diffuse (1×1) hexagonal LEED pattern also emerged using a 57 eV beam as a result of using these cleaning parameters.

A similar plasma exposure at 450 °C (Exp. No. 5, Table II) resulted in a ~0.9 ML reduction in the initial ~2.6 ML of hydroxyls. The Zn $2p_{1/2}$ and Zn $2p_{3/2}$ XPS core-level peaks were shifted from 1044.9 eV and 1021.9 eV for the as-loaded surface to 1044.3 eV and 1021.2 eV for the plasma-cleaned surface; this change in band bending was confirmed by UPS spectral analysis. As shown spectrum (iv) in Fig. 4, the O 1*s* lattice XPS peak showed a 0.4 eV change in band bending through the core-level shift from 530.6 eV for the as-loaded surface to 530.2 eV after cleaning. This change was also confirmed via UPS analysis. The OH peak at 532.3 eV in spectrum (iv) in Fig. 4 is representative of ~1.7 ML of residual OH remaining on the surface. Further analysis showed an increase in the Zn/O ratio from 0.1 for the as-loaded surface to 0.4 for the plasma-cleaned surface. The surface of this particular sample was unpolished; thus, a LEED pattern was not observed. It should be noted that surface polishing (or the lack of it) was not found to influence either the XPS or the UPS results.

Increasing the temperature to 475 °C (Exp. No. 6, Table II) resulted in a reduction of the residual hydroxide by ~0.8 ML. AFM studies did not reveal evidence of thermal decomposition. The O_2/He volume ratio was adjusted to 20%/80% at this temperature. This ratio was determined to be sufficient to suppress desorption of lattice oxygen, while providing sufficient free oxygen radicals to chemically interact with the surface. The XPS spectra showed a 0.7 eV core-level shift in binding energy based on the changes in the Zn $2p$ multiplet from 1022.1 eV and 1045.2 eV for the as-loaded surface to 1021.4 eV and 1044.5 eV after cleaning. The O 1*s* lattice peak for the as-loaded surface was located at 530.9 eV, while the hydroxide signal was detected at 532.8 eV. A 0.5 eV shift in the O 1*s* lattice peak to 530.4 eV was measured after cleaning, as shown in spectrum (v) in Fig. 4. The suppressed companion hydroxide spectrum was located at 532.1 eV. The average core-level shift between the Zn $2p$ and the O 1*s* spectra indicated a 0.6 eV change in band bending associated with the removal of surface contaminants, which correlated to an increase in the Zn/O ratio from 0.4 for the as-loaded surface to 0.8 for the cleaned surface. A (1×1) hexagonal LEED pattern with sharp spots and minimal background was observed at 50 eV.

UPS spectra of the as-loaded ZnO($000\bar{1}$) surface showed that the 3*d* bulk feature is located at 11.2 eV below the Fermi level.[25] The Fermi level was located 0.1 eV above the conduction-band minimum (CBM), giving rise to 0.4 eV of downward band bending at the surface due to the electron accumulation layer described in Sec. I. This behavior and associated charge transfer process have been reported in previous work for ZnO contaminated by the chemisorption of water (and presumably the formation of the hydroxide).[27] In comparison, the flat-band condition for *n*-type ZnO places the Fermi level at 0.3 eV below the CBM.[25,27]

The 475 °C remote plasma cleaning resulted in a sharper valence-band turn on and more distinct bulk features in the spectra for ZnO. An electron affinity[21,23] of 4.4 ± 0.2 eV was deduced from the width of the spectrum. Extrapolation of the valence-band maximum (VBM) from the leading edge of the spectra resulted in a value of 2.7 eV below the Fermi level.

The O $2p$ peak emerged at 4.1 eV below the Fermi level, while the Zn $3d$ feature shifted 0.7 eV to 10.5 eV below the Fermi level. Also, the surface Fermi level shifted down to 0.7 eV below the CBM, indicating upward band bending of 0.4 eV. Overall, these results indicate a 0.8 ± 0.1 eV shift upwards in band bending, which agree with the XPS result of 0.6 ± 0.1 eV.

Significant amounts of the hydroxide were removed from the ZnO$(000\bar{1})$ surface at 500 °C, 525 °C, 575 °C, and 600 °C, as shown in Table II and in spectra (vi) and (vii) for the exposures at 500 °C and 525 °C, respectively, in Fig. 4. The hydroxide was completely removed from the $(000\bar{1})$ surfaces heated at or above 575 °C; however, they now possessed needles associated with thermal decomposition, which were similar in microstructure to the surfaces of samples annealed in oxygen at 700 °C. Thus, the plasma cleaning temperature was set at 525 °C, the O_2 /He ratio, plasma pressure, and plasma power were maintained at 20%/80%, 0.050 Torr, and 20 W, respectively, and the time of exposure to the plasma increased to determine the optimum value.

The optimal plasma exposure time was determined to be 30 min, as processing for 45 min at 525 °C did not result in a decrease in the measurable hydroxide concentration. The optimized plasma clean at 525 °C caused both a shift in the lattice O core-level peak from 530.7 eV to a final position of 530.3 eV, as shown in spectrum (vii) in Fig. 4, and a reduction in the OH concentration. This change in band bending is expected to lead to a reduction in surface conductivity. Approximately 0.4 ML of the OH remained, as derived from the peak at 532.4 eV shown in spectrum (vii) in Fig. 4. A related core-level shift of 0.6 eV for Zn $2p$ was observed with the Zn multiplet moving from 1021.9 eV and 1044.9 eV to 1021.3 eV and 1044.4 eV, respectively. This significant removal of ~1.2 ML of the OH was critical for eliminating the proposed accumulation layer[13,27] and for generating a Zn/O stoichiometric ratio of 1.0 ± 0.1.

The UPS results shown in Fig. 5 also show a 0.5 eV change in band bending, which are in agreement with the XPS results noted above. It is shown in spectrum (i) in Fig. 5 that the Zn $3d$ bulk feature for the as-loaded surface is located at 11.3 eV below the Fermi level, while the O $2p$ bulk feature was not discernible.[25] Thus, the Fermi level was located 0.2 eV above the CBM, giving rise to 0.6 eV of downward band bending at the surface. In comparison, and as noted above, the Fermi level for bulk ZnO is located at 0.3 eV below the CBM. Spectrum (ii) in Fig. 5 shows that after cleaning at 525 °C for 30 min, the O $2p$ bulk feature emerged at 4.0 eV, and the Fermi level shifted down to 0.1 eV below the CBM, resulting in 0.1 eV of downward band bending. An electron affinity of 4.1 ± 0.2 eV was calculated for the clean surface, after extrapolating the VBM from the leading edge of the spectra to 3.3 eV below the Fermi level, as shown in spectrum (ii-ii) in the inset in Fig. 5. Furthermore, the 0.6 eV shift of the Zn $3d$ bulk feature to 10.7 eV matched the corresponding change in band bending found in the XPS spectra. The large peak in the high binding energy region of curves (i) and (ii) in Fig. 5 is due to secondary electrons.[14]

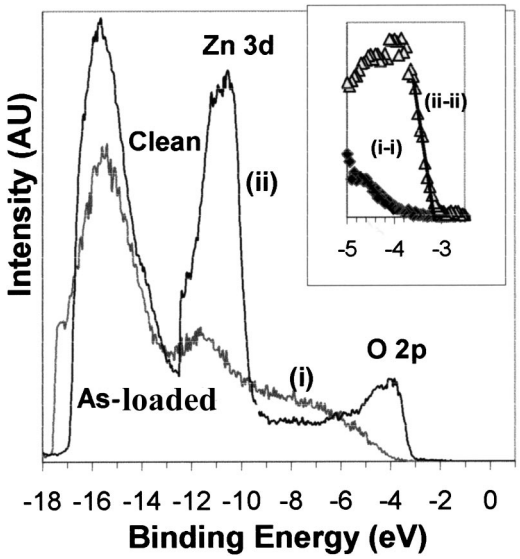

FIG. 5. UPS spectra of ZnO$(000\bar{1})$ surfaces acquired from (i) as-loaded samples and (ii) samples cleaned at 525 °C in a 20 W remote 20% O_2/80% He plasma for 30 min at 0.050 Torr. The inset shows that the valence band turn on for an (i-i) as-loaded sample is sharpened for a (ii-ii) plasma-cleaned surface.

AFM studies revealed the microstructures of the *ex situ* and *in situ* cleaned ZnO$(000\bar{1})$ surfaces, as shown in Figs. 6(a) and 6(b), respectively. The rms roughness values for these respective surfaces were determined to be 0.2 ± 0.2 nm and 0.6 ± 0.2 nm. As shown in Fig 6(b), the cleaning process revealed ordered atomic steps with a unit-cell step height of 0.53 ± 0.01 nm and step width of ~ 0.2 μm. The slight double diffraction of LEED spots observed in the (1×1) hexagonal pattern obtained at 42 eV was likely due to these atomic steps. The propensity for step formation on this surface may also explain similar LEED results reported by Nakagawa and Mitsudo.[15] At energies >42 eV, e.g., 60 eV, only discrete spotswere observed, as the incident beam probed deeper into the ZnO. Very low leakage Schottky con-

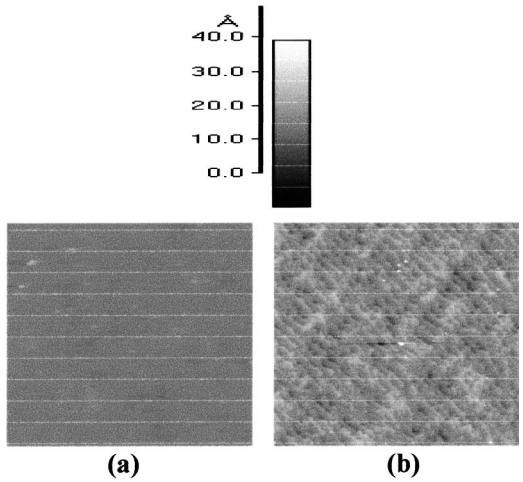

FIG. 6. (5 μm$\times 5$ μm) AFM images of the ZnO$(000\bar{1})$ surface of (a) *ex situ* cleaned samples and (b) samples cleaned at 525 °C via 30 min exposure to a remote 20 W, 20% O_2/80% He plasma at 0.050 Torr.

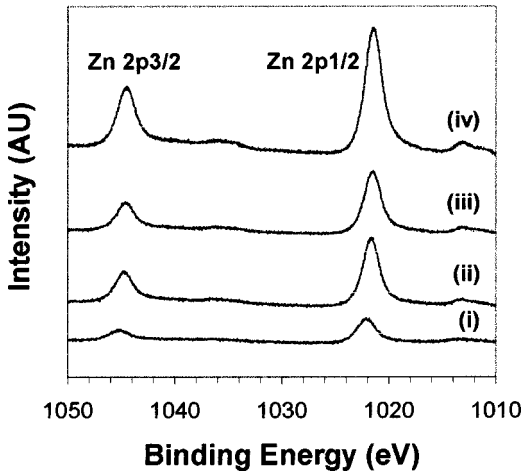

FIG. 7. XPS Zn $2p$ core-level spectra of the Zn(0001) surface acquired from (i) as-loaded samples and samples separately heated to (ii) 525 °C for 30 min, (iii) 525 °C for 60 min, (iv) 550 °C for 60 min and cleaned for these times in a remote 20 W, 20% O_2/80% He plasma at 0.050 Torr.

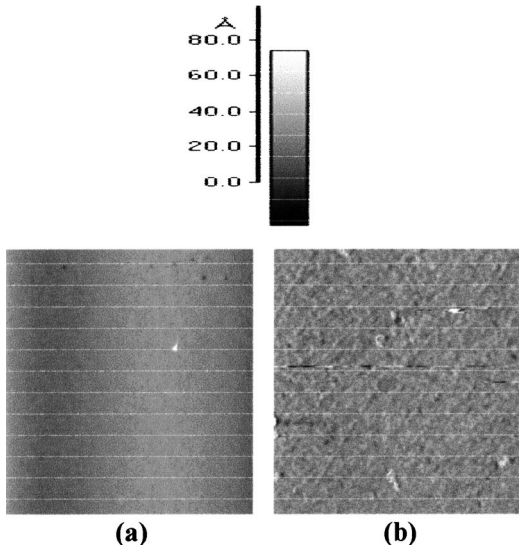

FIG. 8. ($5\ \mu m \times 5\ \mu m$) AFM images of the ZnO(0001) surface of (a) an as-loaded sample and (b) a sample cleaned at 550 °C via 60 min exposure to a remote 20 W, 20% O_2/80% He plasma at 0.050 Torr.

tacts with low ideality factors were also deposited on this optimally cleaned surface by the present authors, as reported elsewhere.[28]

D. Remote plasma cleaning of the ZnO(0001) surface

LEED of the ZnO(0001) surface of the initial sample showed only a bright background, indicative of a disordered contamination layer. Deconvolution of the O 1*s* core-level peak at 532.9 eV and associated calculations revealed that this surface contained ~2.0 ML of OH and that the Zn/O ratio=0.3. The initial investigations to determine the effective cleaning procedure for this surface employed the optimal plasma parameters developed for the $(000\bar{1})$ surface for periods of 30 and 60 min (Exp. Nos. 1 and 2, Table III). The XPS results acquired after these plasma exposures are shown in spectra (ii) and (iii) in Fig. 7. Approximately 1.6 ML of OH remained on the surface, the Zn/O ratio=0.5 and diffuse (1×1) hexagonal LEED patterns were obtained. The hydroxide was more tightly bound to this surface, and this effect was attributed to the presence of unfilled dangling bonds on ZnO(0001).[29,30] The temperature of the plasma exposure was increased only 25 °C to avoid evaporation.

The optimal cleaning procedure employed a 20% O_2/80% He remote plasma at 550 °C and 0.050 Torr for 60 min, followed by evacuation at and cooling from 425 °C. The XPS spectra revealed a shift in the lattice O core-level peak from 530.9 [full width at half maximum (FWHM) =1.6 eV] for the as-loaded surface to 530.4 eV (FWHM =1.4 eV) for the plasma-cleaned surface—a 0.5 eV change in band bending that was again confirmed by UPS investigations. These results also showed ~0.4 ML of OH remaining, as the sole contaminant with a peak at 532.7 eV. A comparison of spectrums (i) and (iv) in Fig. 7 show the corresponding core-level shift of 0.6 eV in the Zn $2p_{1/2}$ and Zn $2p_{3/2}$ peaks from 1022.0 eV and 1045.1 eV (both FWHM =2.3 eV) to 1021.4 eV and 1044.5 eV (both FWHM =2.1 eV), respectively. Figure 7 also indicates the increased intensity of the Zn $2p$ core level after the successive plasma exposures, relative to that acquired from the as-loaded wafers in spectrum (i). Satellite peaks were commonly observed at approximately 1013.2 eV and 1036.2 eV.

This significant removal of ~1.2 ML of the OH was again critical for reducing the proposed accumulation layer[13,14] and for generating a surface with a Zn/O stoichiometric ratio of 1.0. The UPS spectra of the clean ZnO(0001) surface directly matched the cleaned ZnO$(000\bar{1})$ surface, indicating the lack of polarity effects on the electronic structure of a comparably clean surface.

Prior and postcleaning AFM analyses of the (0001) surface confirmed the absence of any observable damage associated with the annealing and/or plasma exposure. A smooth ZnO(0001) microstructure was observed, as shown in Figs. 8(a) and 8(b) with average rms surface roughness values of 1.2 ± 0.2 nm and 1.7 ± 0.2 nm before and after the cleaning process, respectively. The removal of hydroxide from the surface reveals the actual microstructure and corresponding features, and may explain the slight increase in surface roughness. A step-and-terrace microstructure was not observed after cleaning, in contrast to that observed on the cleaned $(000\bar{1})$ surface. Sharp (1×1) hexagonal LEED patterns were obtained at 50 eV. Low leakage Schottky contacts with low ideality parameters were also produced on this surface after cleaning.[31]

The use of the remote O_2/He plasma allowed the operation of both the Langmuir–Hinshelwood (LH) and Eley–Rideal mechanisms.[32] Excited oxygen atoms and molecules produced in the plasma extracted both the hydrocarbons and the hydroxide from the {0001} surfaces without measurable thermal accommodation on these surfaces during cleaning. The LH mechanism was apparently dominant, since the level of adsorbed oxygen on either face was determined to be below the detection limit of XPS. The time dependent nature of the hydroxide removal from ZnO may also be indicative of an LH mechanism, where an intrinsic surface process is as-

sociated with the surface residence time of the oxygen species interacting with the ZnO surface.

IV. SUMMARY

It was determined primarily from XPS spectra that a contamination layer containing an average of 1.0 ML of carbon and averages of 1.5 ML and 1.9 ML of hydroxide is present on the $(000\bar{1})$ and the (0001) surfaces of ZnO and is the reason for the diffuse LEED patterns acquired from these surfaces. Annealing the ZnO$(000\bar{1})$ surface in pure O_2 at 700 °C and 0.1 Torr for 30 min was effective for desorbing the adventitious carbon and the hydroxide below the detection limits ($\sim$0.03 ML) of our XPS system. However, thermal decomposition degraded the surface microstructure and necessitated the development of an alternative approach.

Smooth stoichiometric ZnO$(000\bar{1})$ surfaces having an ordered crystallography, a step-and-terrace microstructure, and nearly flat electronic bands were achieved by exposure to a 20 W remote 20% O_2/80% He plasma for the optimized time, temperature, and pressure of 30 min, 525 °C, and 0.050 Torr, as confirmed by AFM, LEED, XPS, and UPS investigations. Only $\sim$0.4 ML of hydroxide remained as the sole contaminant. This cleaning process also generated a 0.5 eV change in band bending and a significant reduction in the electron accumulation layer, which has been associated primarily with the presence of hydroxide on the surface.

The hydroxide was more tightly bound to the ZnO(0001) surface, which has been attributed to the presence of unfilled dangling bonds associated with the polarity of ZnO{0001} surfaces. This effect increased the temperature and time of the plasma cleaning process to obtain nearly identical results relative to the ZnO$(000\bar{1})$ surface. The optimum cleaning procedure also employed a 20% O_2/80% He remote plasma at 0.050 Torr; however, the temperature and time had to be increased to 550 °C and 60 min, respectively. Similar changes were achieved in the structural, chemical, and electronic properties of this surface. The roughness of the cleaned surface increased slightly relative to the as-received surface; however, step-and-terrace features were not observed.

ACKNOWLEDGMENTS

This research was partially funded by both the Kenan Institute for Technology, Engineering, and Science at NCSU and by the Office of Naval Research under Contract No. N00014-98-1-0654 (H. Dietrich, monitor). The authors express their appreciation to Gene Cantwell, David Eason of Eagle-Picher, Inc., and Aloysius Gonzaga for helpful discussions. One of the authors (R.D.) was partially supported by a Kobe Steel Ltd. Professorship.

[1] W. Göpel, L. J. Brillson, and C. F. Brucker, J. Vac. Sci. Technol. **17**, 894 (1980).
[2] D. C. Look, Mater. Sci. Eng., B **80**, 383 (2001).
[3] F. D. Auret, S. A. Goodman, M. Hayes, M. J. Legodi, H. A. van Laarhoven, and D. C. Look, J. Phys.: Condens. Matter **13**, 1 (2001).
[4] T. Fukumura, Z. Jin, M. Kawasaki, T. Shono, T. Hasegawa, S. Koshihara, and H. Koinuma, Appl. Phys. Lett. **78**, 958 (2001).
[5] S. W. King, J. P. Barnak, M. D. Bremser, K. M. Tracy, C. Ronning, R. F. Davis, and R. J. Nemanich, J. Appl. Phys. **84**, 9 (1998).
[6] R. P. Vasquez, B. F. Lewis, and F. J. Grunthaner, Appl. Phys. Lett. **42**, 293 (1983).
[7] M. Yamada and Y. Ide, Jpn. J. Appl. Phys., Part 2 **33**, L671 (1994).
[8] C. M. Rouleau and R. M. Park, J. Appl. Phys. **73**, 4610 (1993).
[9] L. Fiermans, E. Arijs, J. Vennik, and Vorst, Surf. Sci. **39**, 357 (1973).
[10] H. Jacobs, W. Mokwa, D. Kohl, and G. Heiland, Surf. Sci. **160**, 217 (1985).
[11] M. Mintas and G.W. Filby, Z. Naturforsch. A **36**, 140 (1981).
[12] S. Roberts and R. J. Gorte, J. Chem. Phys. **93**, 5337 (1990).
[13] V. E. Henrich and P. A. Cox, *The Surface Science of Metal Oxides* (Cambridge University Press, Cambridge, UK, 1994), p. 297.
[14] H. Moormann, D. Kohl, and G. Heiland, Surf. Sci. **100**, 302 (1980).
[15] G. Heiland and P. Kunstmann, Surf. Sci. **13**, 72 (1969).
[16] C. M. Nakagawa and H. Mitsudo, Surf. Sci. **175**, 157 (1986).
[17] D. C. Look, D. C. Reynolds, J. R. Sizelove, R. L. Jones, C. W. Litton, G. Cantwell, and W. C. Harsch, Solid State Commun. **105**, 399 (1998).
[18] T. L. Tansley and D. F. Neely, Thin Solid Films **121**, 95 (1984).
[19] R. J. Collins and D. G. Thomas, Phys. Rev. **112**, 388 (1958).
[20] J. van der Weide, Ph.D. dissertation, North Carolina State University, 1994.
[21] D. Briggs and M. P. Seah, *Practical Surface Analysis*, 2nd ed., Appendices (Wiley, New York, 1990).
[22] I. R. Lauks and M. Green, Surf. Sci. **71**, 735 (1978).
[23] R. Leonard and A. Searcy, J. Chem. Phys. **50**, 5419 (1969).
[24] R. Leonard and A. Searcy, J. Appl. Phys. **42**, 4047 (1971).
[25] D. Kohl, M. Henzler, and G. Heiland, Surf. Sci. **41**, 403 (1974).
[26] J. Nowok, Krist. Tech. **11**, 947 (1976).
[27] K. Jacobi, G. Zwicker, and A. Gutmann, Surf. Sci. **141**, 109 (1984).
[28] B. J. Coppa, R. F. Davis, and R. J. Nemanich, Appl. Phys. Lett. **82**, 400 (2003).
[29] V. E. Henrich and P. A. Cox, *The Surface Science of Metal Oxides* (Cambridge University Press, Cambridge, UK, 1994), p. 298.
[30] R. Leysen, G. van Orshaegen, H. van Hove, and A. Neyens, Phys. Status Solidi A **18**, 613 (1973).
[31] B. J. Coppa, C. C. Fulton, R. F. Davis, C. Pandarinath, J. E. Burnette, and R. J. Nemanich (unpublished).
[32] A. Zangwill, *Physics at Surfaces* (Cambridge University Press, Cambridge, UK, 1988), pp. 401–418.